Prognostic significance of peroxiredoxin 1 and ezrin-radixin-moesin-binding phosphoprotein 50 in cholangiocarcinoma

Ponlapat Yonglitthipagon[a,b], **Chawalit Pairojkul**[a,c], **Yaovalux Chamgramol**[a,c], **Alex Loukas**[b], **Jason Mulvenna**[b], **Jeffrey Bethony**[d], and **Banchob Sripa**[a,c,*]

[a]Department of Pathology, Faculty of Medicine, Khon Kaen University, Khon Kaen 40002, Thailand. [b]Queensland Tropical Health Alliance, James Cook University, Cairns, QLD 4878, Australia. [c]Liver Fluke and Cholangiocarcinoma Research Center (LFCRC), Faculty of Medicine, Khon Kaen University. [d]Department of Microbiology, Immunology and Tropical Medicine, George Washington University, Washington, DC 20037, USA.

Summary

We performed a comparative proteomic analysis of protein expression profiles in four cholangiocarcinoma (CCA) cell lines: K100, M156, M213, and M139. The H69 biliary cell line was used as a control. Peroxiredoxin 1 (PRX1) and ezrin-radixin-moesin-binding phosphoprotein 50 (EBP50) were selected for further validation by immunohistochemistry (IHC) using a CCA tissue microarray (n=301) to assess their prognostic value in this cancer. Both PRX1 and EBP50 were overexpressed in CCA tissues compared with normal liver tissues. Of the 301 CCA cases, overexpression of PRX1 in 103 (34.3%) was associated with an age-related effect in young patients ($P = 0.011$) and the absence of cholangiocarcinoma in lymphatic vessels and perineural tissues ($P = 0.004$ and $P = 0.037$, respectively). Expression of EBP50 correlated with histopathologic type, being higher in 180 (59.8%) of moderately or poorly differentiated tumors ($P = 0.039$) and was associated with the presence of cholangiocarcinoma in lymphatic and vascular vessels ($P < 0.001$ and $P < 0.001$, respectively). The high expression of EBP50 and the low expression of PRX1 correlated with reduced survival by univariate analysis ($P = 0.017$ and $P = 0.048$, respectively). Moreover, the impact of PRX1 and EBP50 expression on patient survival was an independent predictor in multivariate analyses ($P = 0.004$ and $P = 0.025$, respectively). Therefore, altered expression of PRX1 and EBP50 may be used as prognostic markers incholangiocarcinoma.

Keywords

Cholangiocarcinoma; EBP50; Proteomics; PRX1; Prognostic marker; Tumor marker

*Corresponding author. Division of Experimental Pathology, Department of Pathology, Faculty of Medicine, Khon Kaen University, Khon Kaen 40002, Thailand. banchob@kku.ac.th *Tel.:*+66 43 363 113, *Fax:* +66 43 202 024 .

1. Introduction

Cholangiocarcinoma (CCA) is a primary liver cancer occurring in the bile duct epithelium. Although a rare tumor worldwide, CCA has a high incidence in Southeast Asia, especially in northeastern Thailand, where infection with the liver fluke, *Opisthorchis viverrini*, is endemic. This infection is transmitted by the consumption of raw or undercooked freshwater fish in regional dishes that contain the metacercarial (ie, infective) stage of the fluke. Once consumed, the immature flukes migrate up the ampulla of Vater to the biliary tree and mature in the small intrahepatic bile ducts. An estimated 6 million people are infected with *O. viverrini* in Thailand,[1] where it has long been hypothesized that chronic infection with *O. viverrini* is associated with the development of CCA.[2] Indeed, there may be no stronger link between a eukaryotic organism and a malignant neoplasm than that between *O. viverrini* and CCA, which led the World Health Organization's International Agency for Research on Cancer to classify *O. viverrini* as a Group 1 carcinogen.[3]

Advanced CCA has an extremely poor prognosis. Over the past 30 years, much effort has been devoted to improving the survival rate of CCA patients. Surgical resection of all detectable tumors from the liver and bile duct improves the five-year survival rate, but surgical resection must be done before an advanced stage of CCA is reached, and unfortunately, the majority of patients present with advanced CCA, which is not amenable to surgical intervention. Hence, the discovery of novel biomarkers to refine prognosis and response to treatment is of great importance.

Two-dimensional gel electrophoresis (2-DE) and mass spectrometry (MS) are still the method of choice for the analysis of proteins. Although the technique itself is difficult to reproduce and is therefore not applicable as a diagnostic tool, it can be used for the discovery of tumor markers.

Recently, a comparative proteomic study of membrane proteins from four human *O. viverrini*–associated CCA cell lines with a non-tumor H69 biliary cell line as a control identified annexin A2 (ANXA2) as a prognostic marker for the outcome of CCA patients.[4] In the present study, we not only attempted to characterize cytosolic protein profiles from CCA cell lines with different tumor-forming capabilities and a non-tumor H69 biliary cell line, but also to determine the prognostic significance of candidate proteins in the human liver under normal conditions and in CCA.

2. Materials and methods

2.1. Cell lines and cell culture

Four human CCA cell lines, M156, K100, M139, and M213, were isolated from CCA patients from northeastern Thailand, as described elsewhere.[5] In all cases, CCA was associated with chronic *O.viverrini* infection. Approval for use of the tissue was obtained from the Human Research Ethics Committee of Khon Kaen University. The CCA tissues were classified histologically as follows: moderately differentiated adenocarcinoma (M156), poorly differentiated adenocarcinoma (K100), squamous cell carcinoma (M139), and adenosquamous cell carcinoma (M213). The H69 cells, an immortalized non-malignant human cholangiocyte cell line, and the CCA cell lines were cultured as previously described.[4]

2.2. Tissue samples

The CCA tissues were obtained after informed consent from patients who underwent hepatectomy at Srinagarind Hospital, Khon Kaen University, as described elsewhere.[4] Of the 301 liver fluke–associated CCA samples, 203 were from male patients and 98 from

female patients, a ratio of 2:1. The mean (±SD) age in years was 55 ± 9.4 (range 31–75 years). Most of the patients were at an advanced CCA stage, 73.9% (n = 210) with lymphatic invasion, 53.1% (n = 152) with vascular invasion, and 39.6% (n = 112) with perineural invasion. The histopathologic grade of the tumors was assessed as well-differentiated in 53 patients (35%). The majority of the patients (63.5%) possessed a tumor> 5 cm.

2.3. Extraction of cytosolic proteins

The cell lines were examined under a phase-contrast microscope to ensure that they were > 70% confluent before lysis. The culture medium was discarded, and the cells were washed with 0.25 M sucrose three times on ice and scraped thoroughly in 0.25 M sucrose containing 1% Protease Inhibitor Mix (GE Healthcare, Piscataway, NJ USA). The cells were collected and centrifuged at 1,500 $\times g$ for 5 min at 4°C. The pellets were resuspended in lysis buffer (7 M urea, 2 M thiourea, 4% CHAPS, 2% IPG buffer pH 3–10 nonlinear [GE Healthcare], 40 mM DTT, and 1% Protease Inhibitor Mix) on ice for 15 min. Lysis was achieved by sonication on ice (3×5-s pulses). The lysates were clarified by sequential centrifugation at 600 $\times g$ for 10 min to remove the nuclei and unlysed cells, at 10,000 $\times g$ for 15 min to remove the mitochondrial fraction, and at 100,000 $\times g$ for 2 h to generate a pellet containing the enriched microsomal fraction and the supernatant liquid representing the cytosolic fraction. The total protein in the cytosol was quantified by Bradford assay.

2.4. Two-dimensional gel electrophoresis and image analysis

Total protein (100 µg)[Au: correct?] from the CCA cell lines and H69 as a control was separated by 2-DE using IPG strips (pH 3–10NL, 7 cm) as described previously.[4] After electrophoresis, the protein spots were visualized by CBR-250 (GE Healthcare) staining. Stained gels were scanned using an ImageScanner (GE Healthcare), and the 2-DE images of each cell line were compared using ImageMaster 2D Platinum 6.0 software (GE Healthcare).

2.5. In-gel digestion of 2-DE, MALDI-TOF MS analysis and database search

Protein spots that were unique to or stained more intensely in CCA cell lines compared with H69 cells were excised from the gel and transferred to V-bottom 96-well microtiter plates. Tryptic digestions were performed on an Ettan Spot Handling Workstation robot (Amersham Biosciences; a division of GE Healthcare). Matrix solution was prepared by dissolving 10 mg of α-cyano-4-hydroxycinnamic acid (Bruker Daltonik GmbH, Bremen,Germany) to saturation in 50% acetonitrile/water with 0.1% trifluoroacetic acid and then mixing with equal volumes of tryptic peptides. The mixture (1 µL) was spotted on a steel target surface (MTP 384 ground steel; Bruker Daltonik) and dried at room temperature. Mass spectra were recorded on an Autoflex MALDI-TOFmass spectrometer (Bruker Daltonik) at a maximum accelerating potential of 19 kV in the reflector mode. The m/z range was from 400 to 4000. Typically, 100 shots were accumulated from three to five different positions within a sample spot. Proteins were identified by peptide mass fingerprinting (PMF) using Mascot (http://www.matrixscience.com) in searches against the NCBInr 2009.04.03 database. The parameters used in the Mascot searches were as follows: (1) taxonomy was restricted to *Homo sapiens*; (2) trypsin was specified with the allowance for one missed cleavage; (3) peptide mass tolerance and fragment mass tolerance were set to 100 ppm and □ 0.5 Da, respectively; and (4) carbamidomethyl and oxidized methionine were chosen as the fixed and variable modifications, respectively. Protein hits were considered significant if the Mascot score was > 43 (significance $P< 0.05$). Other criteria for confident identification were that the protein match should have at least 17% sequence coverage and match at least 11 peptides. If peptides matched multiple members of a protein

family, proteins with shared peptides were grouped; and the highest scoring protein was selected as the representative.

2.6. Tissue microarray and immunohistochemistry

Tissue microarrays (TMAs) were constructed by the Department of Pathology, Faculty of Medicine, Khon Kaen University. Following TMA construction,[6] a hematoxylin and eosin-stained section of the TMA recipient block was prepared and reviewed to confirm the presence of intact neoplasm. The arrays contained 301 CCA cases and 4 cases of non-tumor liver tissues as control samples. One core was taken from the non-necrotic area of tumor focii in each formalin-fixed paraffin-embedded CCA sample using punch cores that measured 0.9 mm in greatest diameter. Prior to TMA construction, all tissue slides were re-evaluated by an experienced histopathologist (C.P.). The extent of invasion by the cancer was determined in both the interface of the growing tumor border and the adjacent liver tissue. Pathologic *vascular invasion* was defined as the presence of a tumor embolus within a vessel space, identified by associated fibrin clot or an endothelial cell lining. *Lymphatic invasion* was defined as present when cancer cells were floating within an endothelium-lined space. *Perineural invasion* was defined as tumor invading the perineural sheath or endoneurium.

Immunohistochemical (IHC) reactions were performed on 4-μm-thick sections of TMA silane-coated slides (Sigma, St. Louis, MO, USA) by an immunoperoxidase method as described.[4] The TMA sections probed with rabbit polyclonal anti-peroxiredoxin 1 (Abcam Inc., Cambridge, MA USA) diluted 1:500 (v/v) or rabbit polyclonal anti-EBP50 (Abcam) diluted 1:400 (v/v) in PBS and incubated overnight at 4°C. After rinsing for 3×5 min with PBS, the sections were incubated at room temperature for 1 h with biotin-conjugated goat anti-rabbit immunoglobulin (Zymed Laboratories, San Francisco, CA) diluted 1:300 (v/v) in PBS. The sections were then incubated at room temperature for 1 h with horseradish peroxidase-conjugated streptavidin (Zymed Labs) diluted 1:300 (v/v) in PBS. Sections were rinsed with PBS for 2×10 min, after which they were developed with DAB (Sigma). The sections were counterstained with Mayer's hematoxylin, dehydrated, cleared in xylene, and mounted in Permount.

2.7. Immunohistochemical and statistical analysis

Immunoreactivity was evaluated independently by three researchers (P.Y., B.S., and C.P.), who were blinded to patient status and outcome. Consensus was reached whenever disagreement occurred. The percentage of positive tumor cells was determined using interactive stereologic immunoscoring based on systematic random sampling,[7] and the average score was calculated. More specifically, within a defined area of the lesion, we randomly selected five high-power fields (magnification 400×; 100 cells/field), and approximately 500 tumor cells were counted. The percentage of positive cells expressing PRX1 and EBP50 was categorized as <10% (−) or 10% (+), as described elsewhere.[8]

For cross-sectional analyses, the χ^2 test was utilized to analyze the relation between PRX1 and EBP50 expression and categorical variables regarding clinical pathology parameters (eg, age group, sex, and histologic type). The Kaplan–Meier method was used to calculate cumulative survival. Differences in survival between the low-expression and high-expression groups were analyzed for significance by the log-rank method. The Cox regression model was used to perform multivariate analysis, and the results were considered of statistical significance if the *P* value was < 0.05. The statistical analysis was performed using SPSS 16.0 (SPSS, Inc, Chicago, IL USA).

3. Results

3.1. 2-DE profiling of proteins differentially expressed in H69 and CCA cells

In order to examine the differential protein expression profiles of CCA cell lines, three biological replicates for each cell type (M156, KKU100, M139, M213, and H69) were generated. The separated protein spots were visualized on 2D gels by CBR-250 staining and displayed good reproducibility for spot quantification and comparative analysis. Figure 1 shows representative 2-DE maps of each CCA cell line (M156, K100, M139, and M213) with spots subjected to MALDI-TOF MS and their identification numbers; the identified spots are listed in Table 1. The experimental pI and Mr values of identified proteins correlated with the theoretical values reported in the NCBInr database. As reported previously,[4] some differences observed between the experimental and theoretical pI/Mr values and the presence of different isoforms of the same protein could reflect post-translational modifications or splice variants.

3.2. Protein identification by MALDI-TOF MS

Using 2D gel replicates, the identical and differential protein expression in four CCA cell lines subtracted from H69 was measured. In Table 1, the proteins, corresponding to 48 spots expressed in CCA cell lines but not in H69, are shown, together with the MS identification parameters. To classify the biological significance of the differentially expressed proteins, MS-identified proteins were classified into molecular and biological functional groups using the PANTHER database. Several of the proteins identified have been associated with cancer in previous studies,[9–12] such as HSP60 and HSP70/HSP90, enolase-alpha, and hnRNPs. As illustrated in Figure 2, MALDI-TOF MS analysis and peptide mass fingerprinting of the tryptic digests subsequently identified protein spot 38 as PRX1 (Fig. 2A), spot 39 as ezrin (Fig. 2B), and spot 40 as moesin (Fig. 2C). Peroxiredoxin 1 (PRX1) and EBP50, a binding partner of ezrin and moesin, were selected for further verification, as their degree of expression correlates with tumor progression in other cancers,[13,14] but their prognostic utilities in human *O. viverrini*-associated CCA have not been explored.

3.3. Immunohistochemistry of PRX1 and EBP50

Immunohistochemistry analysis was carried out on the TMA ($n = 301$) using anti-PRX1 and anti-EBP50 rabbit polyclonal antibodies to confirm PRX1 and EBP50 expression changes during cholangiocarcinogenesis. Weak staining of PRX1 (Fig. 3A) and EBP50 (Fig. 3B) were observed in the cytoplasm and on the apical surface of normal hepatocytes and cholangiocytes. In contrast, PRX1 (Fig. 3C) and EBP50 (Fig. 3D) were highly expressed in the majority of the corresponding CCA tissues, concentrated in the cytoplasm with moderate labeling on the apical surface. Expression of EBP50 and PRX1 was found in the biopsies from 180 patients (59.8%) and 103 patients (34.3%), respectively. Statistical analysis showed that overexpression of PRX1 was associated with an age-related effect in young CCA patients (56 years; $P = 0.001$), and an absence of lymphatic ($P = 0.004$) and perineural ($P = 0.037$)invasion, whereas EBP50 was associated with tumor invasion ($P = 0.039$), particularly in lymphatic ($P<0.001$) and blood vessels ($P<0.001$), as shown in Table 2.

3.4. PRX1 and EBP50 expression and cumulative survival

When the variables statistically significant in the univariate analyses were included in a Cox proportional hazard analysis, moderately or poorly differentiated histologic type (hazard ratio, 1.56; $P = 0.0015$), overexpression of EBP50 (hazard ratio, 1.37; $P = 0.025$), and underexpression of PRX1 (hazard ratio, 1.51; $P = 0.004$) were identified as independent predictors of patient survival (Table 3). The median length of survival for patients with high

PRX1 expression was 38 weeks (95% confidence interval [CI] 26.10, 49.90 weeks), and 29 weeks (95% CI 23.47, 34.53 weeks) for patients with low PRX1 expression. In contrast, the median survival for patients with high EBP50 expression was 27.14 weeks (95% CI 21.68, 32.60 weeks) and 38.57 weeks (95% CI 27.16, 49.99 weeks) for patients with low EBP50 expression (Table 3). Survival curves for the patients were categorized on the basis of the PRX1 and EBP50 staining categories and are displayed in Figure 4. Diminished survival was seen in cases with high expression of EBP50 ($P = 0.017$) and low expression of PRX1 ($P = 0.048$).

4. Discussion

Identification of protein profiles is important for understanding the mechanisms of cholangiocarcinogenesis and could facilitate the development of new tools for the diagnosis, treatment, and prevention of CCA. We applied a proteomics-based approach to identify differentially expressed tumor proteins in CCA cell lines. Upregulation of peroxiredoxin 1 (PRX1), ezrin, and moesin in moderately differentiated (M156), but not in poorly differentiated (K100), CCA cell lines might imply association with a better prognosis. However, a drawback of this method is that cell lines are not representative of the tissue of origin,as they have been propagated *in vitro* for extended time periods.[15] Furthermore, each cell line was established from a few cells of a single patient biopsy; hence, these lines may not accurately represent the overall tumor characteristics.[15] Accordingly, validation of comparative proteomic results from the cell lines in the biopsies is an important step in developing prognostic markers for CCA. Therefore, PRX1 and EBP50 were selected for further verification using IHC analysis on TMA of CCA tissues.

Peroxiredoxins are found in mammals, yeast, and bacteria and are characterized as thiol-specific antioxidant proteins. They are further classified as possessing either one or two conserved cysteine residues.[16] The catalytic mechanism of the 2-Cys peroxiredoxins, particularly PRX1, is specific among the peroxide-detoxifying enzymes.[17] The function of PRX1 in particular has been implicated as regulating cell proliferation, differentiation, and apoptosis.[18]

Upregulation of PRX1 has been linked to tumor suppression in oral squamous cell cancer and low PRX1 expression with larger tumor masses, lymph node metastases, and poorly differentiated cancers.[19] However, the connection between PRX1 and bile duct cancer has not been clearly defined. Our IHC analysis showed an association between the overexpression of PRX1 in human *O. viverrini*–associated CCA and a decrease in tumor invasion of lymphatic and vascular vessels. PRX1 is an antioxidant associated with the cell's defenses against oxidative damage.[20] Pinlaor et al.[21] suggested a model of inflammation-mediated cholangiocarcinogenesis progressing via NO-mediated oxidative and nitrative DNA damage in hamsters infected with *O. viverrini.* Therefore, it is reasonable to suggest that the overexpression of PRX1 seen in our study is explained by increased production of reactive oxygen species in CCA tissue.

Furthermore, we have identified ezrin and moesin, members of the ezrin-radixin-moesin (ERM) family, which have been reported as a ligand for EBP50 or Na^+/H^+ exchanger regulatory factor.[25]The EBP50 protein is an adapter molecule containing two tandem post-synaptic density-95/disk-large/ZO-1 homologous (PDZ) domains that can bind integral membrane proteins and the N-terminal ERM association domain (N-ERMAD) of ERM proteins,[14] promoting the assembly of membrane-bound macromolecular complexes involved in signal transduction.[26]

Although EBP50 was first hypothesized to be a mitogenic factor, it was later shown to act as an oncogene[27,28] or a tumor suppressor gene,[29,30]depending on its location in the cells. Recently,investigators report that EBP50 acts as a tumor suppressor by interacting with β–catenin and stabilizing adherent junctions or forming a triple complex with phosphatase and tensin homolog (PTEN) and platelet-derived growth factor receptor on the cell membrane of epithelial cells, thereby exerting an inhibitory action on PI3K signaling.[31] However, overexpression and intracellular delocalization of EBP50 can break up complexes with PTEN or β-catenin and also scaffold complexes in the cytoplasm or nucleus, thus promoting tumor progression by separating signaling molecules from the plasma membrane.[32] In addition, EBP50 has been reported to be overexpressed and redistributed to the cytoplasmor nucleus or both of proliferative cells in hepatocellular carcinoma[28] and in estrogen-stimulated tissues such as endometrium and breast cancers.[27,33] Consistent with this possibility, we found that overexpression of EBP50 was clearly visible in both the cytoplasm and the membrane of CCA tissues, and its expression was associated with tumor invasion of lymphatic and blood vessels.

A Cox regression model (Table 3) showed that PRX1, EBP50, histologic type, and tumor invasion were associated with longer survival after surgery. More specifically, patients with low expression of EBP50 and high expression of PRX1 had longer survival after surgery than patients with high expression of EBP50 and low expression of PRX1. In the case of tumor invasion and metastasis, it has been reported that the survival after surgery for the group with tumor invasion and metastasis was shorter than in the group without tumor invasion and metastasis in CCA,[34] which is further supported by our findings. In addition, the expression pattern we reportis in accordance with previous findings that patients with well-differentiated CCA have longer survival times after surgery compared with those havingthe moderately or poorly differentiated type.[35]

5. Conclusions

This study has characterized for the first time the elevated expression of PRX1 and EBP50 and their correlations with the clinicopathological parameters and overall survival. Our results indicate that dysregulation of EBP50 and PRX1 may serve as a prognostic marker for CCA.

Acknowledgments

References

[1]. Sripa B, Sithithaworn P, Sirisinha S. *Opisthorchis viverrini* and opisthorchiasis: the 21st century review. Acta Trop. 2003; 88:169–70. [PubMed: 14611870]

[2]. Sripa B, Kaewkes S, Sithithaworn P, et al. Liverfluke induces cholangiocarcinoma. PLoS Med. 2007; 4:e201. [PubMed: 17622191]

[3]. Bouvard V, Baan R, Straif K, et al. A review of human carcinogens B: biological agents. Lancet Oncol. 2009; 10:321–2. [PubMed: 19350698]

[4]. Yonglitthipagon P, Pairojkul C, Chamgramol Y, Mulvenna J, Sripa B. Up-regulation of annexin A2 in cholangiocarcinoma caused by *Opisthorchis viverrini* and its implication as a prognostic marker. Int J Parasitol. 2010; 40:1203–12. [PubMed: 20493868]

[5]. Sripa B, Leungwattanawanit S, Nitta T, et al. Establishment and characterization of an opisthorchiasis-associated cholangiocarcinoma cell line (KKU-100). World J Gastroenterol. 2005; 11:3392–7. [PubMed: 15948244]

[6]. Fedor HL, De Marzo AM. Practical methods for tissue microarray construction. Methods Mol Med. 2005; 103:89–101. [PubMed: 15542899]

[7]. van Diest PJ, van Dam P, Henzen-Logmans SC, et al. A scoring system for immunohistochemical staining: consensus report of the Task Force for Basic Research of the EORTC-GCCG. European Organization for Research and Treatment of Cancer-Gynaecological Cancer Cooperative Group. J Clin Pathol. 1997; 50:801–4. [PubMed: 9462258]

[8]. Zhuang PY, Zhang JB, Zhu XD, et al. Two pathologic types of hepatocellular carcinoma with lymph node metastasis with distinct prognosis on the basis of CK19 expression in tumor. Cancer. 2008; 112:2740–8. [PubMed: 18412155]

[9]. Zhong L, Peng X, Hidalgo GE, Doherty DE, Stromberg AJ, Hirschowitz EA. Antibodies to HSP70 and HSP90 in serum in non-small cell lung cancer patients. Cancer DetectPrevent. 2003; 27:285–90.

[10]. Desmetz C, Bibeau F, Boissiere F, et al. Proteomics-based identification of HSP60 as a tumor-associated antigen in early stage breast cancer and ductal carcinoma in situ. JProteome Res. 2008; 7:3830–7. [PubMed: 18683965]

[11]. Chang YS, Wu W, Walsh G, Hong WK, Mao L. Enolase-alpha is frequently down-regulated in non-small cell lung cancer and predicts aggressive biological behavior. Clin Cancer Res. 2003; 9:3641–4. [PubMed: 14506152]

[12]. David CJ, Chen M, Assanah M, Canoll P, Manley JL. HnRNP proteins controlled by c-Myc deregulate pyruvate kinase mRNA splicing in cancer. Nature. 463:364–8. [PubMed: 20010808]

[13]. Kim JH, Bogner PN, Ramnath N, Park Y, Yu J, Park YM. Elevated peroxiredoxin 1, but not NF-E2-related factor 2, is an independent prognostic factor for disease recurrence and reduced survival in stage I non-small cell lung cancer. Clin Cancer Res. 2007; 13:3875–82. [PubMed: 17606720]

[14]. Song J, Bai J, Yang W, Gabrielson EW, Chan DW, Zhang Z. Expression and clinicopathological significance of oestrogen-responsive ezrin-radixin-moesin-binding phosphoprotein 50 in breast cancer. Histopathology. 2007; 51:40–53. [PubMed: 17593079]

[15]. Hay, MM.; Chen, TR.; McClintock, P.; Reid, Y. American Type Culture Collection Catalogue of Cell Lines and Hybridomas. 6th ed. ATCC; Rockville, Md: 1988.

[16]. Rhee SG, Kang SW, Chang TS, Jeong W, Kim K. Peroxiredoxin, a novel family of peroxidases. IUBMB Life. 2001; 52:35–41. [PubMed: 11795591]

[17]. Kim YJ, Lee WS, Ip C, Chae HZ, Park EM, Park YM. Prx1 suppresses radiation-induced c-Jun NH2-terminal kinase signaling in lung cancer cells through interaction with the glutathione S-transferase Pi/c-Jun NH2-terminal kinase complex. Cancer Res. 2006; 66:7136–42. [PubMed: 16849559]

[18]. Cha MK, Suh KH, Kim IH. Overexpression of peroxiredoxin I and thioredoxin1 in human breast carcinoma. J Exp Clin Cancer Res. 2009; 28:93. [PubMed: 19566940]

[19]. Yanagawa T, Iwasa S, Ishii T, et al. Peroxiredoxin I expression in oral cancer: a potential new tumor marker. Cancer Lett. 2000; 156:27–35. [PubMed: 10840156]

[20]. Chang JW, Jeon HB, Lee JH, et al. Augmented expression of peroxiredoxin I in lung cancer. BiochemBiophysResCommun. 2001; 289:507–12.

[21]. Pinlaor S, Hiraku Y, Ma N, et al. Mechanism of NO-mediated oxidative and nitrative DNA damage in hamsters infected with *Opisthorchis viverrini*: a model of inflammation-mediated carcinogenesis. Nitric Oxide. 2004; 11:175–83. [PubMed: 15491850]

[22]. Wu XY, Fu ZX, Wang XH. Peroxiredoxins in colorectal neoplasms. HistolHistopathol. 2010; 25:1297–303.

[23]. Berggren MI, Husbeck B, Samulitis B, Baker AF, Gallegos A, Powis G. Thioredoxin peroxidase-1 (peroxiredoxin-1) is increased in thioredoxin-1 transfected cells and results in enhanced protection against apoptosis caused by hydrogen peroxide but not by other agents including dexamethasone, etoposide, and doxorubicin. ArchBiochemBiophys. 2001; 392:103–9.

[24]. Kim SY, Kim TJ, Lee KY. A novel function of peroxiredoxin 1 (Prx-1) in apoptosis signal-regulating kinase 1 (ASK1)-mediated signaling pathway. FEBS Lett. 2008; 582:1913–8. [PubMed: 18501712]

[25]. Reczek D, Berryman M, Bretscher A. Identification of EBP50: a PDZ-containing phosphoprotein that associates with members of the ezrin-radixin-moesin family. J Cell Biol. 1997; 139:169–79. [PubMed: 9314537]

[26]. Maudsley S, Zamah AM, Rahman N, et al. Platelet-derived growth factor receptor association with Na^+/H^+ exchanger regulatory factor potentiates receptor activity. Mol Cell Biol. 2000; 20:8352–63. [PubMed: 11046132]

[27]. Cardone RA, Bellizzi A, Busco G, et al. The NHERF1 PDZ2 domain regulates PKA-RhoA-p38-mediated NHE1 activation and invasion in breast tumor cells. Mol Biol Cell. 2007; 18:1768–80. [PubMed: 17332506]

[28]. Shibata T, Chuma M, Kokubu A, Sakamoto M, Hirohashi S. EBP50, a beta-catenin-associating protein, enhances Wntsignaling and is over-expressed in hepatocellular carcinoma. Hepatology. 2003; 38:178–86. [PubMed: 12830000]

[29]. Lazar CS, Cresson CM, Lauffenburger DA, Gill GN. The Na^+/H^+ exchanger regulatory factor stabilizes epidermal growth factor receptors at the cell surface. Mol Biol Cell. 2004; 15:5470–80. [PubMed: 15469991]

[30]. Kreimann EL, Morales FC, de Orbeta-Cruz J, et al. Cortical stabilization of beta-catenin contributes to NHERF1/EBP50 tumor suppressor function. Oncogene. 2007; 26:5290–9. [PubMed: 17325659]

[31]. Pan Y, Weinman EJ, Dai JL. Na^+/H^+ exchanger regulatory factor 1 inhibits platelet-derived growth factor signaling in breast cancer cells. Breast Cancer Res. 2008; 10:R5. [PubMed: 18190691]

[32]. Georgescu MM. NHERF1: molecular brake on the PI3K pathway in breast cancer. Breast Cancer Res. 2008; 10:106. [PubMed: 18430260]

[33]. Stemmer-Rachamimov AO, Wiederhold T, Nielsen GP, et al. NHE-RF, a merlin-interacting protein, is primarily expressed in luminal epithelia, proliferative endometrium, and estrogen receptor-positive breast carcinomas. Am J Pathol. 2001; 158:57–62. [PubMed: 11141479]

[34]. Uttaravichien T, Bhudhisawasdi V, Pairojkul C, Pugkhem A. Intrahepatic cholangiocarcinoma in Thailand. J Hepato-Biliary-Pancreatic Surg. 1999; 6:128–35.

[35]. Nathan H, Pawlik TM, Wolfgang CL, Choti MA, Cameron JL, Schulick RD. Trends in survival after surgery for cholangiocarcinoma: a 30-year population-based SEER database analysis. J Gastrointest Surg. 2007; 11:1488–7. [PubMed: 17805937]
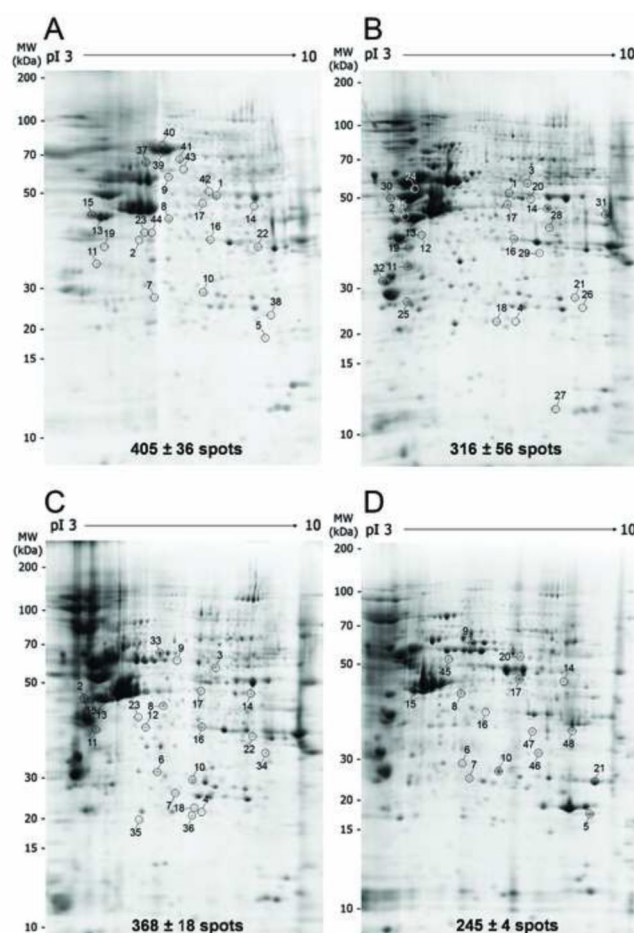
Fig.1.
Two-dimensional electrophoresis maps of cytosolic proteins of four cholangiocarcinoma cell lines: M156, moderately differentiated (A), KKU-100, poorly differentiated (B), M139, squamous cell carcinoma (C), and M213, adenosquamous cell carcinoma (D). Number of spots totaled 405☐36, 316☐56, 368☐18, and 245☐34 (mean±S.E. of three biological replicates) for M156, KKU-100, M139, and M213, respectively.
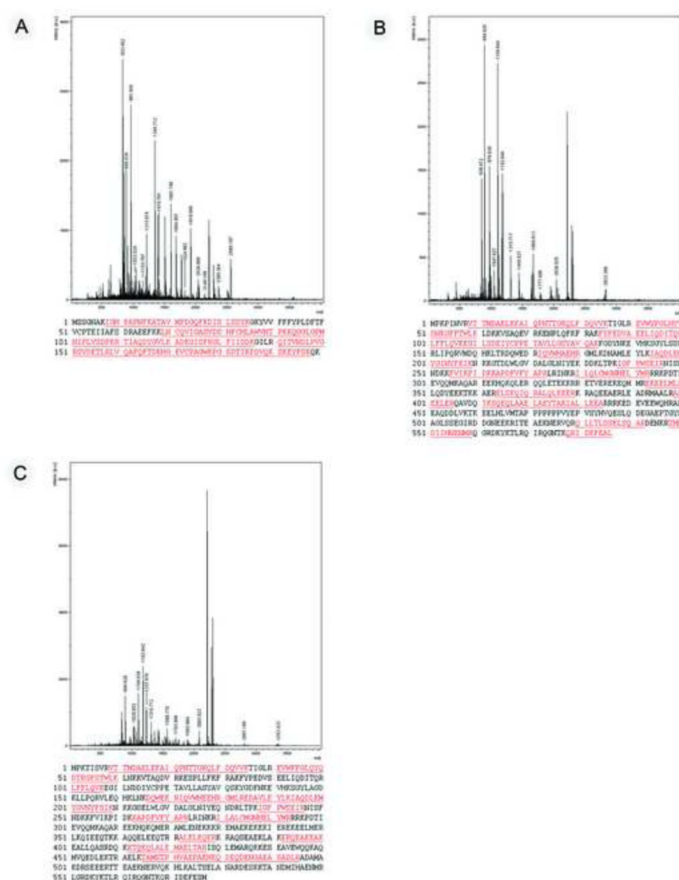
Fig.2.
Peptide mass fingerprint (PMF) of tryptic digests of peroxiredoxin 1 (A), ezrin (B), and moesin (C) obtained by MALDI-TOF MS. The spectrum displays *m/z* ratio (*x*axis) and relative intensity (*y*axis) of the peptides identified. Matched peptides of peroxiredoxin 1, ezrin, and moesin were 76%, 43%, and 33% protein sequence coverage, shown by red and underline, respectively. Protein identification using PMF data was performed with the Mascot search engine; acquired spectra were processed and search against the NCBInr database.
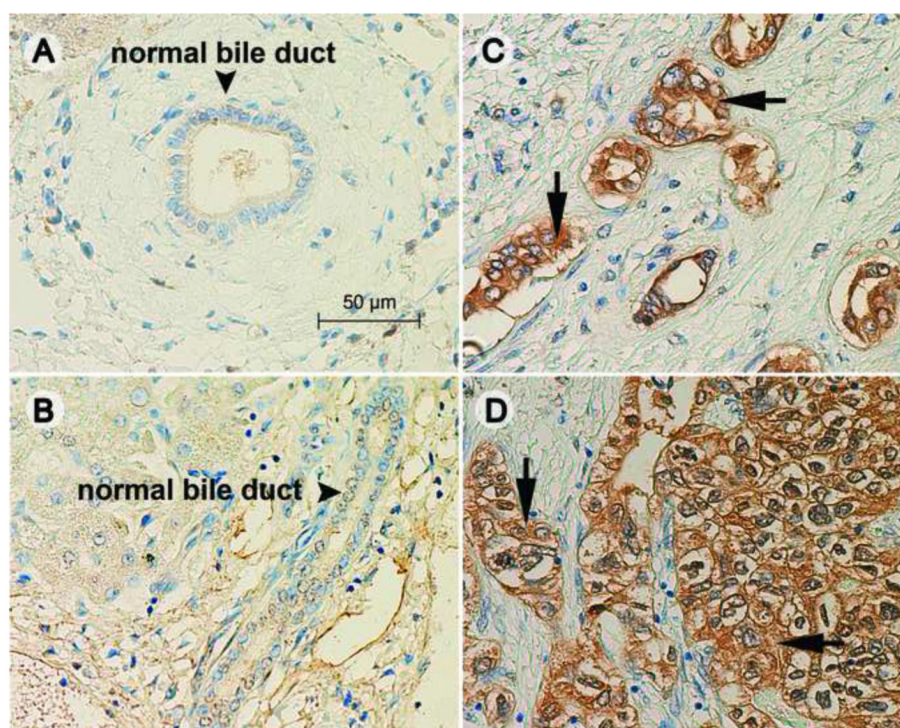
Fig.3.
Immunohistochemistry of peroxiredoxin 1 (PRX1) and ezrin-radixin-moesin-binding phosphoprotein 50 (EBP50) expression in normal bile duct epithelium and cholangiocarcinoma (CCA). Weak expression of PRX1 (A) and EBP50 (B) was found in human normal cholangiocytes (arrowhead), whereas high expression was observed mainly in the cytoplasm and on the apical surface of CCA tissues (arrow). Immunoperoxidase staining, original magnification × 200 (A–D).
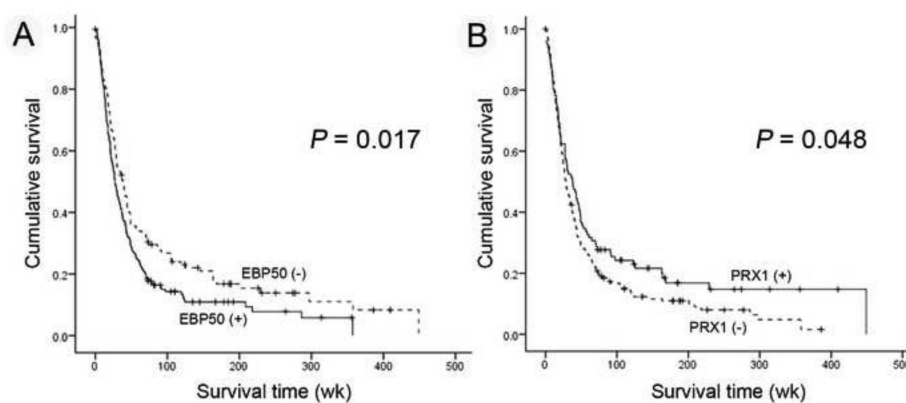
Fig.4.
Kaplan-Meier cumulative curves for overall survival of *Opisthorchis viverrini*-associated cholangiocarcinoma (CCA) patients according to expression of ezrin-radixin-moesin-binding phosphoprotein 50 (EBP50) (A) and peroxiredoxin 1 (PRX1) (B) in primary tumors.

Table 1

Differentially Expressed Cytosolic Proteins from Four CCA Cell Lines Identified by MALDI-TOF MS

| No.ᵃ	A/Nᵇ	Description	Biological process	MSᶜ	MP/TPᵈ	COᵉ	Mr-ᶠ	pIᵍ	H69	M156	K100	M139	M213
1	gi|34147630	Tu translation elongation factor	Signal transduction	194	28 / 38	65	50.19	7.26	−	+	+	−	−
2	gi|1710248	Protein disulfide isomerase	Protein metabolic process	69	7 / 36	17	46.51	4.95	−	−	+	+	−
3	gi|169404695	Chain A, Pyruvate Kinase M2	Carbohydrate metabolic process	185	22 / 51	38	57.09	8	−	−	+	+	−
4	gi|544759	Biliverdin-IX beta reductase isozyme I	Unknown	110	10 / 27	51	21.96	7.31	−	−	+	+	−
5	gi|5031635	Cofilin 1	Cellular component morphogenesis	202	18 / 55	75	18.72	8.22	−	+	−	−	+
6	gi|4505773	Prohibitin	Nucleic and nucleotide metabolic process	211	17 / 42	73	29.84	5.57	−	+	−	+	+
7	gi|4758638	Peroxiredoxin 6	Oxygen and reactive oxygen species metabolic process	147	17 / 50	79	25.13	6	−	+	−	+	+
8	gi|119581639	Proteasome	Protein metabolic process	240	28 / 53	65	43.22	5.97	−	+	−	+	+
9	gi|4502643	Chaperonin containing TCP1	Protein metabolic process	306	38 / 80	65	58.44	6.23	−	+	−	+	+
10	gi|999892	Triosephosphate Isomerase	Carbohydrate metabolic process	220	19 / 42	84	26.81	6.51	−	+	−	+	+
11	gi|18314408	Nucleophosmin	Nucleic and nucleotide metabolic process	78	11 / 50	27	32.73	4.59	−	+	+	+	−
12	gi|15277503	ACTB protein	Cellular component morphogenesis	164	21 / 44	67	40.54	5.35	−	+	+	+	−
13	gi|62897681	Calreticulin	Protein metabolic process	222	20 / 38	58	47.06	4.3	−	+	+	+	−
14	gi|48145549	PGK1	Carbohydrate metabolic process	354	36 / 46	62	44.97	8.3	−	+	+	+	+
15	gi|90111766	Keratin 19	Cellular component organization	375	34 / 49	75	44.08	5.04	−	+	+	+	+
16	gi|119582950	Annexin A1	Intracellular protein transport	252	28 / 45	77	40.48	6.57	−	+	+	+	+
17	gi|203282367	Enolase 1	Carbohydrate metabolic process	174	21 / 44	53	47.35	6.99	−	+	+	+	+
18	gi|3023905	Glutathione S-transferase	Immune system process	148	12 / 34	57	23.64	6.89	−	−	+	+	−

No.[a]	A/N[b]	Description	Biological process	MS[c]	MP/TP[d]	CO[e]	M_r[f]	pI[g]	H69	M156	K100	M139	M213
19	gi|4502107	Annexin 5	Signal transduction	176	17 / 27	54	35.97	4.94	–	+	+	–	–
20	gi|197210452	Uridine monophosphate synthetase	Unknown	95	11 / 53	16	52.71	6.81	–	–	+	–	+
21	gi|4503727	FK506 binding protein 3, 25kDa	Negative regulation of apoptosis	109	12 / 38	44	25.22	9.26	–	–	+	–	+
22	gi|67464043	Human liver Gapdh	Carbohydrate metabolic process	185	19 / 29	57	36.48	8.53	–	+	–	+	–
23	gi|82195535	Gamma-actin	Cellular component morphogenesis	165	22 / 50	64	42.09	5.3	–	+	–	+	–
24	gi|119602173	Heat shock protein 90kDa	Response to stress	117	16 / 35	27	57.87	4.92	–	–	+	–	–
25	gi|4507651	Tropomyosin 4 isoform 2	Cellular component organization	146	14 / 31	43	28.62	4.67	–	–	+	–	–
26	gi|21620034	ZSCAN21 protein	Nucleic and nucleotide metabolic process	43	12 / 20	24	26.69	9.45	–	–	+	–	–
27	gi|46409504	Hypothetical protein LOC400165	Unknown	46	42 / 82	38	13.69	8.66	–	–	+	–	–
28	gi|123266507	Guanylatecyclase 1, soluble, beta 2	Nucleic and nucleotide metabolic process	44	39 /56	19	44.95	8.84	–	–	+	–	–
29	gi|7669492	Glyceraldehyde-3-phosphate dehydrogenase	Carbohydrate metabolic process	67	42 / 55	18	36.21	8.57	–	–	+	–	–
30	gi|5174735	Tubulin, beta, 2	Intracellular protein transport	148	23 / 36	57	50.26	4.79	–	–	+	–	–
31	gi|7108915	Glucocorticoid receptor AF-1	Signal transduction	69	42 / 85	19	46.58	9.08	–	–	+	–	–
32	gi|49119653	YWHAZ protein	Signal transduction	153	16 / 37	45	30.11	4.72	–	–	+	–	–
33	gi|189502784	Heat shock protein 60kD	Response to stress	249	30 / 48	59	60.81	5.83	–	–	–	+	–
34	gi|4504447	hnRNP A2/B1	Intracellular protein transport	89	19 / 46	44	36.04	8.67	–	–	–	+	–
35	gi|4507669	Tumor protein, translationally controlled 1	Immune system process	116	16 / 41	61	19.69	4.84	–	–	–	+	–
36	gi|55960374	Transgelin 2	Muscle contraction	88	10 / 31	45	21.24	7.63	–	–	–	+	–
37	gi|31542947	Chaperonin	Protein metabolic process	230	26 / 50	52	61.19	5.7	–	+	–	–	–
38	gi|4505591	Peroxiredoxin 1	Oxygen and reactive oxygen species	243	19 / 33	76	22.32	8.27	–	+	–	–	–

No.[a]	A/N[b]	Description	Biological process	MS[c]	MP /TP[d]	CO[e]	Mr[f]	pI[g]	H69	M156	K100	M139	M213
			metabolic process										
39	gi|46249758	Ezrin	Intracellular protein transport	258	28 / 31	43	69.31	5.94	–	+	–	–	–
40	gi|4505257	Moesin	Intracellular protein transport	146	26 / 46	33	67.89	6.08	–	+	–	–	–
41	gi|5803181	Hsp70/Hsp90	Response to stress	129	38 / 85	55	63.23	6.4	–	+	–	–	–
42	gi|52632385	hnRNP L	Nucleic and nucleotide metabolic process	104	13 / 28	35	51.16	7.22	–	+	–	–	–
43	gi|38013966	TKT protein	Lipid metabolic process	303	22 / 26	46	58.74	6.51	–	+	–	–	–
44	gi|167860126	Serine proteinase inhibitor	Protein metabolic process	278	25 / 42	73	42.53	5.72	–	+	–	–	–
45	gi|12803727	Keratin 7	Cellular component organization	210	22 / 33	46	51.44	5.42	–	–	–	–	+
46	gi|42476281	Voltage-dependent anion channel 2	Ion transport	147	13 / 25	54	32.06	7.49	–	–	–	–	+
47	gi|5174447	Guanine nucleotide binding protein	Intracellular protein transport	225	21 / 32	56	35.51	7.61	–	–	–	–	+
48	gi|54303910	Aging-associated gene 9 protein	Carbohydrate metabolic process	155	14 / 27	43	36.19	8.57	–	–	–	–	+

Note: The presence of a protein in the relevant study is denoted with a '+' and the absence with a '–'.

[a] numbers correspond to Figure 1

[b] NCBInr database accession numbers

[c] Mascot score (MS = −10×Log (P) where P is the probability that the observed match is a random event from MS analysis

[d] the number of matched peaks/total peaks in MS analysis

[e] percentage of sequence coverage

[f] molecular weight

[g] isoelectric point

Table 2

Clinicopathological Variables and Expression Status of Peroxiredoxin 1 (PRX1) and Ezrin-Radixin-Moesin-Binding Phosphoprotein 50 (EBP50) in Cholangiocarcinoma Tissues

Variables	EBP50			PRX1		
	–ve	+ve	*p*	–ve	+ve	*p*
Age (yrs)						
56	69	100	NS	101	68	0.011
> 56	55	75		96	34	
Sex						
Male	79	124	NS	137	66	NS
Female	44	51		59	36	
Histotype group						
Less diff.	104	134	0.039	158	80	NS
Well diff.	15	38		35	18	
Gross type						
Mass forming	60	85	NS	94	51	NS
Periductal infiltrating	22	39		44	17	
Intraductal	5	4		6	3	
Tumor size (cm)						
5	29	45	NS	47	27	NS
> 5	55	74		80	49	
Vascular invasion						
Absent	75	59	<0.001	90	44	NS
Present	44	108		100	52	
Lymphatic invasion						
Absent	44	30	<0.001	39	35	0.004
Present	75	135		149	61	
Perineural invasion						
Absent	71	100	NS	103	68	0.037
Present	48	64		85	27	

Note: When the sum of subset numbers does not match patient totals, data were missing or unavailable. Tumor invasion in cholangiocarcinoma (CCA) tissues was diagnosed as positive if the patient fulfilled one of these three criteria: (1) vascular invasion; (2) lymphatic invasion; or (3) perineural invasion. NS indicates that the χ^2 is not significant using the 0.05 threshold.

Table 3

Clinical Risk Factors for Overall Survival in Cholangiocarcinoma

Risk factor	Overall survival					
	Univariate analysis (Log-rank)		Multivariate analysis (Cox regression)			
	Median time, wk ± SE (95% CI)	p	Relative risk	95% CI	p	
Histology						
Well differentiated	41.14 ± 6.47 (28.47, 53.81)	0.029	1	0.44, 0.92	0.015	
Less differentiated	29.00 ± 2.63 (23.85, 34.15)		1.56			
Gender						
Male	27.14 ± 1.74 (23.74, 30.54)	0.025	1.29	0.97, 1.71	NS	
Female	40.14 ± 4.22 (31.86, 48.42)		1			
PRX1 expression						
Low	29.00 ± 2.82 (23.47, 34.53)	0.048	1.511	1.14, 2.01	0.004	
High	38.00 ± 6.07 (26.10, 49.90)		1			
EBP50 expression						
Low	38.57 ± 5.82 (27.16, 49.99)	0.017	1	0.56, 0.96	0.025	
High	27.14 ± 2.79 (21.68, 32.60)		1.37			

Abbreviations: CI, confidence interval; NS, not significant.